

### Scaled-Factorial-Moment Analysis of 200A-GeV Sulfur +Gold Interactions

M. I. Adamovich,<sup>(12)</sup> M. M. Aggarwal,<sup>(14)</sup> Y. A. Alexandrov,<sup>(12)</sup> Z. V. Ameeva,<sup>(15)</sup> N. P. Andreeva,<sup>(15)</sup> Z. V. Anzon,<sup>(15)</sup> R. Arora,<sup>(14)</sup> S. K. Badyal,<sup>(3)</sup> K. B. Bhalla,<sup>(2)</sup> A. Bhasin,<sup>(3)</sup> V. S. Bhatia,<sup>(14)</sup> V. I. Bubnov,<sup>(15)</sup> T. H. Burnett,<sup>(11)</sup> X. Cai,<sup>(7)</sup> I. Y. Chasnikov,<sup>(15)</sup> L. P. Chernova,<sup>(13)</sup> M. M. Chernyavski,<sup>(12)</sup> B. Dressel,<sup>(9)</sup> G. Z. Eligbaeva,<sup>(15)</sup> L. E. Eremenko,<sup>(15)</sup> E. M. Friedlander,<sup>(10)</sup> S. I. Gadzhieva,<sup>(13)</sup> A. S. Gaitinov,<sup>(15)</sup> E. R. Ganssaug,<sup>(9)</sup> S. Garpman,<sup>(8)</sup> S. G. Gerassimov,<sup>(12)</sup> A. Gill,<sup>(2)</sup> J. G. Grote,<sup>(11)</sup> K. G. Gulamov,<sup>(13)</sup> U. G. Gulyamov,<sup>(1)</sup> V. K. Gupta,<sup>(3)</sup> S. Hackel,<sup>(9)</sup> H. H. Heckman,<sup>(10)</sup> H. Haung,<sup>(7)</sup> B. Judek,<sup>(4)</sup> S. Kachroo,<sup>(3)</sup> F. G. Kadyrov,<sup>(13)</sup> G. S. Kalyachkina,<sup>(15)</sup> E. K. Kanygina,<sup>(15)</sup> G. L. Kaul,<sup>(3)</sup> M. Kaur,<sup>(14)</sup> S. P. Kharlamov,<sup>(12)</sup> T. Koss,<sup>(11)</sup> V. Kumar,<sup>(2)</sup> P. Lal,<sup>(2)</sup> V. G. Larionova,<sup>(12)</sup> P. J. Lindstrom,<sup>(10)</sup> L. S. Liu,<sup>(7)</sup> S. Lokanathan,<sup>(2)</sup> J. J. Lord,<sup>(11)</sup> N. S. Lukicheva,<sup>(13)</sup> S. B. Luo,<sup>(5)</sup> N. V. Maslennikova,<sup>(12)</sup> L. K. Mangotra,<sup>(3)</sup> I. S. Mitra,<sup>(14)</sup> S. Mookerjee,<sup>(2)</sup> C. Mueller,<sup>(9)</sup> S. H. Nasyrov,<sup>(1)</sup> V. S. Navotny,<sup>(13)</sup> G. I. Orlova,<sup>(12)</sup> I. Otterlund,<sup>(8)</sup> N. G. Peresadko,<sup>(12)</sup> S. Persson,<sup>(8)</sup> N. V. Petrov,<sup>(1)</sup> W. Y. Qian,<sup>(7)</sup> R. Raniwala,<sup>(2)</sup> S. Raniwala,<sup>(2)</sup> N. K. Rao,<sup>(3)</sup> J. T. Rhee,<sup>(9)</sup> N. A. Salmanova,<sup>(12)</sup> W. Schultz,<sup>(9)</sup> C. I. Shakhova,<sup>(15)</sup> V. S. Shukla,<sup>(2)</sup> B. Singh,<sup>(14)</sup> D. Skelding,<sup>(11)</sup> K. Soderstrom,<sup>(8)</sup> E. Stenlund,<sup>(8)</sup> S. C. Strausz,<sup>(11)</sup> J. F. Sun,<sup>(5)</sup> L. N. Svechnikova,<sup>(13)</sup> M. I. Tretyakova,<sup>(12)</sup> H. Q. Wang,<sup>(7)</sup> Z. Q. Weng,<sup>(5)</sup> R. J. Wilkes,<sup>(11)</sup> G. F. Xu,<sup>(6)</sup> D. H. Zhang,<sup>(5)</sup> P. Y. Zheng,<sup>(6)</sup> D. C. Zhou,<sup>(7)</sup> and J. C. Zhou<sup>(7)</sup>

<sup>(1)</sup>*Institute of Nuclear Physics, Tashkent 700084, U.S.S.R.*

<sup>(2)</sup>*University of Jaipur, Jaipur 302004, India*

<sup>(3)</sup>*University of Jammu, Jammu 18004, India*

<sup>(4)</sup>*National Research Council, Ottawa, Ontario, Canada K1A 0R6*

<sup>(5)</sup>*Shanxi Normal University, Linfen, People's Republic of China*

<sup>(6)</sup>*Institute of High Energy Physics, Beijing, People's Republic of China*

<sup>(7)</sup>*Hua-Zhong Normal University, Wuhan, People's Republic of China*

<sup>(8)</sup>*University of Lund, Lund S-22362, Sweden*

<sup>(9)</sup>*Phillipps University, Marburg D-3550, Federal Republic of Germany*

<sup>(10)</sup>*Lawrence Berkeley Laboratory, Berkeley, California 94720*

<sup>(11)</sup>*University of Washington, Seattle, Washington 98195*

<sup>(12)</sup>*Lebedev Institute of Physics, Moscow 117924, U.S.S.R.*

<sup>(13)</sup>*Physical-Technical Institute, Tashkent 700084, U.S.S.R.*

<sup>(14)</sup>*Panjab University, Chandigarh 160014, India*

<sup>(15)</sup>*Institute of High Energy Physics, Alma-Ata, U.S.S.R.*

(Received 29 March 1990)

S+Au interactions at 200A GeV were observed using emulsion chambers, permitting measurement of pseudorapidities in the central region with precision  $\sim 0.01$  unit. Scaled-factorial-moment analyses are extended to bin sizes smaller than those accessible to other fixed-target experimental techniques. For a sample of 151 central collisions, moments are calculated using both "horizontal" and "vertical" analysis techniques. While the moments are found to rise (in a log-log plot) with decreasing pseudorapidity bin size  $\delta\eta$ , their slopes roll off to approximately zero for  $\delta\eta < 0.1$ .

PACS numbers: 25.70.Np, 12.40.Ee, 13.85.Hd, 24.60.Ky

An important feature of central ultrarelativistic heavy-ion collisions is the presence of significant fluctuations in rapidity density. This phenomenon has been seen both in cosmic-ray experiments<sup>1</sup> and in accelerator experiments.<sup>2</sup> It has been suggested that a quark-gluon plasma phase transition could give rise to such behavior. Other collective phenomena such as minijet formation may also lead to large fluctuations. Therefore, analysis of the properties of fluctuations is important, Białas and Peschanski<sup>3,4</sup> introduced the method of scaled factorial moments (SFMs), which was shown to give results independent of statistical fluctuations inherent in finite data samples. The behavior of the moments may reveal fundamental features of the particle production process.<sup>5,6</sup>

EMU01 emulsion chambers were exposed to 200A-GeV sulfur ions at CERN in October 1987. The chambers of seven parallel 780- $\mu\text{m}$ -thick polystyrene plates coated on both sides with Fuji ET7B emulsion. The chambers were oriented during exposure such that sulfur beam entered normal to the plates. The target layer was a 250- $\mu\text{m}$ -thick gold foil immediately upstream of the second emulsion plate. In contrast to the conventional emulsion pellicle technique, tracks can be readily separated for measurement and the amount of matter in the path of produced particles is negligible so that secondary interactions and Coulomb scattering are minimized. Most experimental results, including those presented here, measure the pseudorapidity  $\eta_i = -\ln \tan(\theta_i/2)$ , where  $\theta_i$  is the laboratory production angle of track  $i$ ,

rather than true rapidity. Tracks with production angles  $\theta_i < 30^\circ$  ( $\eta > 1.32$ ) are detected with nearly 100% efficiency. Repeated measurements indicate a precision of approximately 0.01 pseudorapidity unit in the central region,  $2 < \eta < 4$ , in contrast to conventional emulsion pellicle techniques which typically have a resolution limit of  $\sim 0.1$ . Details of the chamber design and data-reduction procedures have been given elsewhere.<sup>7-9</sup>

The present analysis focuses on central collisions, i.e., interactions in which essentially all projectile nucleons participate. Events were selected which contained fewer than three singly charged minimum-ionizing particles within 1 mrad of the beam direction and no projectile fragments with charge  $Z > 1$ . This cut simulates the effects of small-angle veto triggers in other experiments, permitting intercomparison of data. Simulation studies employing the Lund Monte Carlo program<sup>10</sup> FRITIOF show that it efficiently selects central collisions. Results presented here are from a sample of 151 S+Au events which meet these criteria. The average charged multiplicity (for minimum-ionizing particles with  $\eta \geq 1.32$ ) was  $\langle n_s \rangle = 355$ .

The pseudorapidity range  $\Delta\eta$  is divided into  $M$  bins of

$$\langle F_q \rangle_H = \frac{1}{N_{\text{events}}} \sum_{i=1}^{N_{\text{events}}} M^{q-1} \sum_{m=1}^M \frac{k_{m,i}(k_{m,i}-1) \cdots (k_{m,i}-q+1)}{\langle N \rangle^q}, \quad (2)$$

where  $N_{\text{events}}$  is the number of events in the sample,  $k_{m,i}$  is the content of bin  $m$  in event  $i$ , and  $\langle N \rangle$  is the average multiplicity in pseudorapidity window  $\Delta\eta$ . Results using this mode of analysis<sup>11</sup> suggest power-law behavior of moments down to the experimental resolution limit  $\delta\eta = 0.1$ .

With the horizontal analysis, all of the bins are treated uniformly, so some of the variation in the factorial moments is due to  $\eta$  dependence of the average multiplicity within a bin. The pseudorapidity density distribution is far from uniform, as can be seen in the typical  $\eta$  distribution shown in Fig. 1. To correct for this variation, one may adopt an alternate approach referred to as the "vertical" analysis,<sup>12</sup> in which

$$\langle F_q \rangle_V = \frac{1}{M} \sum_{m=1}^M \frac{1}{N_{\text{events}}} \sum_{i=1}^{N_{\text{events}}} \frac{k_{m,i}(k_{m,i}-1) \cdots (k_{m,i}-q+1)}{\langle k_m \rangle^q}. \quad (3)$$

Here,

$$\langle k_m \rangle = N_{\text{events}}^{-1} \sum_{i=1}^{N_{\text{events}}} k_{m,i}, \quad (4)$$

the average content of bin  $m$  over the ensemble of events, is substituted for  $\langle N/M \rangle$ . In this formulation the factorials are weighted by the average multiplicity for a given bin rather than the overall average bin multiplicity.

For both horizontal and vertical procedures, we find that the  $\langle F_q \rangle$  exhibit a rise consistent with a power-law dependence upon  $\delta\eta$  for larger bin sizes, but with slopes (on the conventional log-log plot) rolling off to approximately zero near  $\delta\eta = 0.1$  (Figs. 2 and 3). Error bars represent the standard deviation of  $F_q$  over all events and all bins used. Point-to-point variations in the plots appear to be small compared to the error bars because the points represent successive rebinning of the same data and are therefore strongly correlated.

For a large sample of central S+Au events generated

uniform width  $\delta\eta = \Delta\eta/M$ . For a single event containing  $N$  tracks in the window  $\Delta\eta$ , the  $q$ th scaled factorial moment is

$$F_q = M^{q-1} \sum_{m=1}^M \frac{k_m(k_m-1) \cdots (k_m-q+1)}{N(N-1) \cdots (N-q+1)}, \quad (1)$$

where  $k_m$  is the number of particles in the  $m$ th bin. The behavior of  $F_q$  as a function of  $\delta\eta$  (hence of  $M$ ) is an indicator of the correlation length for fluctuations. For example, one might expect an increase in  $F_q$  with decreasing  $\delta\eta$  until  $\delta\eta$  is chosen to be smaller than the scale length for fluctuations, at which point  $F_q$  would become independent of  $\delta\eta$ .

The preceding calculation applies to single events, but in practice it is necessary to average over an ensemble of events. Equation (1) can be generalized to include events of varying multiplicity in several ways. The simplest approach is to use Eq. (1) averaged over the event sample, i.e., an exclusive average. This procedure neglects the influence of varying multiplicities on the SFMs, so an inclusive average, where  $N(N-1) \cdots (N-q+1)$  is replaced with  $\langle N \rangle^q$ , has been the preferred method. The latter approach is referred to as the "horizontal" analysis. The moments are then given by

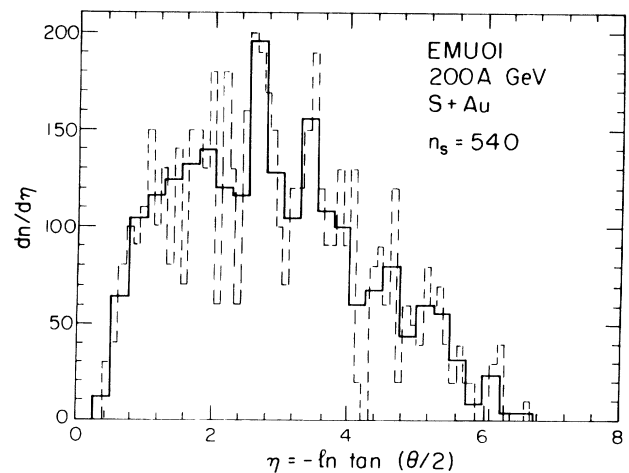


FIG. 1. Pseudorapidity distribution for a typical central 200A-GeV S+Au interaction. Two versions are shown to illustrate the bin-size dependence of apparent fluctuations. Solid histogram: 0.25 unit/bin; dashed histogram: 0.10 unit/bin.

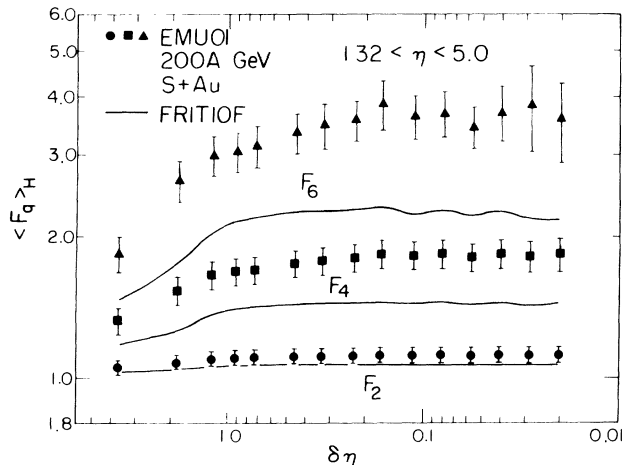


FIG. 2. Scaled factorial moments for a sample of 151 central S+Au interactions using the “horizontal” (inclusive) analysis in the window  $1.32 < \eta < 5.0$ . The second, fourth, and sixth moments are shown, along with corresponding results from a large sample of equivalent events generated by FRITIOF. Magnitudes of the FRITIOF moments differ from those of the data due to a slightly different multiplicity distribution within the pseudorapidity window  $\Delta\eta$ .

by the Monte Carlo program FRITIOF, only the  $\langle F_q \rangle_H$  display a bin-size dependence, as shown in Fig. 2. The  $\langle F_q \rangle_V$  for the FRITIOF events remain constant, independent of  $\delta\eta$ . We conclude that the rise in the  $\langle F_q \rangle_H$  as a function of decreasing  $\delta\eta$  is in large part due to the overall shape of the pseudorapidity density distributions. FRITIOF includes conventional short-range correlations, so the initial rise in the experimental moments at large  $\delta\eta$  cannot be due to, e.g., decay of resonances. We included the effects of  $\gamma$  conversion in the gold target, but even with the added  $e^+e^-$  pairs, the vertical moments for FRITIOF data remained flat.

We have also investigated the dependence of the SFMs upon pseudorapidity window size and location, and upon event multiplicities. Because of space limitations, we must leave these results for a forthcoming full length paper.<sup>13</sup>

Fiałkowski *et al.*<sup>14</sup> showed that the horizontal moments can be corrected for the nonuniform shape of the rapidity distributions by dividing by the factor

$$R_F = \frac{1}{M} \sum_{m=1}^M M^q \frac{\langle k_m \rangle^q}{\langle N \rangle^q}. \quad (5)$$

Horizontal moments corrected in this way are compared with the corresponding vertical moments in Fig. 3. The correction procedure should be used with some caution, since it is derived under the assumption that the argument of the outer summation in Eq. (3) is independent of bin location; this assumption is valid only for relatively small windows in the central region, and substantial variation may occur for windows approaching the target and projectile fragmentation regions. In the following

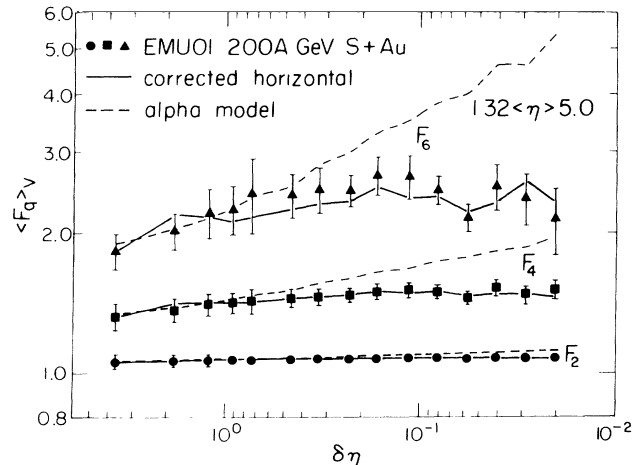


FIG. 3. SFMs for the same data set and window as in Fig. 2, using the “vertical” analysis. For comparison, the solid line shows the results of the horizontal analysis for the experimental data (as in Fig. 2), corrected using the procedure of Fiałkowski *et al.* (Ref. 14). The dashed line shows the vertical analysis results for a sample of events generated by the alpha model (see text). Error bars on the data represented by the solid and dashed lines are comparable or smaller than those shown on the vertical analysis points. FRITIOF results (not shown) in the vertical analysis are flat for all moments considered.

discussion we shall concentrate on the vertical analysis results, although, as shown in Fig. 3, the corrected horizontal data for the windows used are in generally good agreement.

As seen in Fig. 3,  $\ln\langle F_q \rangle_V$  rises with decreasing bin size but the slope rolls off to approximately zero. Note that other reported results from fixed-target experiments have resolution limits typically corresponding to  $\sim 0.1$  in  $\delta\eta$  and thus do not probe the entire region discussed here. When we use the limited range  $\delta\eta > 0.1$ , our results are in general agreement with those of other experiments; i.e., the data suggest uniform log-linear behavior. We have not fitted slopes to these data, since the slopes obtained depend strongly upon the windows used.

It is well known that linear dependence of  $\ln\langle F_q \rangle_V$  on  $\ln\delta\eta$  is a signature of intermittent behavior, but one expects that for events of finite multiplicity, the linear behavior must eventually turn over at sufficiently small  $\delta\eta$ , where bins become sparsely populated. As a test of our sensitivity to finite multiplicity effects at small  $\delta\eta$ , we generated events using the alpha model introduced by Białas and Peschanski<sup>3,4</sup> as an example of intermittency.

The alpha model is a procedure for producing a statistical distribution containing fluctuations which scale uniformly as a power law down to an arbitrarily small scale chosen by the resolution of the simulation. An initial uniform particle density distribution is repeatedly subdivided, with self-similar fluctuations imposed independently upon each subdivision for each partitioning.

After the final partition, experimental noise is simulated by selecting the number of tracks in each bin from a Poisson distribution with mean value given by the model output. Figure 3 also shows moments calculated for such simulated events, with a multiplicity distribution equivalent to that of our experimental sample, generated with model parameters  $\alpha=0.27$ ,  $\beta=0.1$ , and  $\nu=10$ , where  $\beta$  gives the probability per iteration for the occurrence of a positive fluctuation of relative magnitude  $\alpha$  and  $\nu$  is the number of partitioning steps. The moments for the alpha-model events exhibit consistent power-law behavior down to the smallest inherent scale, showing that our analysis is sensitive to intermittent behavior down to  $\delta\eta=0.02$  even though our data have finite bin populations. However, for the experimental data in Fig. 3, the moments become nearly constant for  $\delta\eta < 0.1$  suggesting a change from the intermittent behavior seen for  $\delta\eta > 0.1$ .

The same analysis was also performed using azimuthal angles  $\phi_i$ . Both the EMU01 data and FRITIOF events showed constant factorial moments within error, indicating that this method shows no nonstatistical fluctuations in the range  $\delta\phi > 0.025$  rad, except for the effects of fluctuations in total multiplicities.

Particle pseudorapidities for a sample of 151 central 200A-GeV S+Au interactions have been measured with precision  $\sim 0.01$  unit, significantly better than that accessible to most other experiments. SFMs of the  $\eta$  distributions, for windows spanning the central region, have been calculated using both the "horizontal" (inclusive) and "vertical" analysis techniques. While the moments exhibit power-law dependence on  $\delta\eta$  for bin widths  $\delta\eta > 0.1$ , i.e.,  $\ln\langle F_q \rangle$  rises with decreasing  $\ln\delta\eta$ , their slopes roll off to approximately zero for  $\delta\eta < 0.1$ . This behavior of the moments indicates that the particle production processes in ultrarelativistic nucleus-nucleus collisions produce nonstatistical fluctuations which manifest themselves in the pseudorapidity distribution on scales down to  $\sim 0.1$  unit of pseudorapidity; i.e., evidence of fluctuations is not observed for smaller scales investigat-

ed,  $0.02 < \delta\eta < 0.1$ . For a similar study of fluctuations in azimuthal angle, no dependence of  $F_q(\phi)$  on  $\delta\phi$  is found.

Thanks are due to R. Peschanski and R. Hwa for helpful discussions, and to the scanning and measuring personnel within the collaboration. We gratefully acknowledge financial support from the Department of Energy under Contract No. DE-AS06-88FR40423-KA010, the National Science Foundation, U.S. Sweden Program, the Swedish Natural Science Research Council, the German Federal Minister of Research and Technology, the National Natural Science Foundation of China, the University Grants Commission, Government of India, and the Distinguished Teacher Foundation of the State Education Commission of China.

<sup>1</sup>T. H. Burnett *et al.*, Phys. Rev. Lett. **50**, 2062 (1983).

<sup>2</sup>E. Stenlund *et al.*, Nucl. Phys. **A498**, 541c (1989).

<sup>3</sup>A. Białas and R. Peschanski, Nucl. Phys. **B273**, 703 (1986).

<sup>4</sup>A. Białas and R. Peschanski, Nucl. Phys. **B308**, 857 (1988).

<sup>5</sup>I. Dremin, Mod. Phys. Lett. A **13**, 1333 (1988); Fermilab report, 1989 (to be published).

<sup>6</sup>P. Carruthers, University of Arizona Report No. AZPH-TH/89-28, 1988 (to be published), and references therein.

<sup>7</sup>M. Adamovich *et al.*, Phys. Lett. B **201**, 397 (1988).

<sup>8</sup>M. Adamovich *et al.*, in *Intersections Between Particle and Nuclear Physics*, edited by G. M. Bunce, AIP Proceedings No. 176 (American Institute of Physics, New York, 1989), p. 1047.

<sup>9</sup>S. Garpman *et al.*, Nucl. Instrum. Methods Phys. Res., Sect. A **269**, 134 (1988).

<sup>10</sup>B. Nilsson-Almqvist and E. Stenlund, Comput. Phys. Commun. **43**, 387 (1987).

<sup>11</sup>R. Holynski *et al.*, Phys. Rev. Lett. **62**, 733 (1989); I. Avijenko *et al.*, Phys. Lett. B **235**, 373 (1989); K. Sengupta *et al.*, Phys. Lett. B **236**, 219 (1990).

<sup>12</sup>R. Peschanski (private communication).

<sup>13</sup>M. Adamovitch *et al.*, University of Washington Report No. VTL-PHY-124 (to be published).

<sup>14</sup>K. Fiałkowski *et al.*, Acta Phys. Pol. B **20**, 639 (1989).